

Shape Tracking using Partial Information Models

Antonio Zea, Florian Faion, and Uwe D. Hanebeck¹

Abstract—One of the challenges in shape tracking is how to deal with associating measurements to sources in the shape, while also taking into account parameters such as shape curvature and noise characteristics. *Partial Information Models* (PIMs) introduce a new approach that addresses this issue. The idea is to reparametrize each measurement into two components, one which depends on the position of its source on the shape, and another which depends on how well it fits in the shape. This allows for the derivation of a partial likelihood which combines the strengths of probabilistic approaches and distance minimization techniques. We propose an implementation of PIMs using level-sets, which allow for a close approximation of the distribution of distances we expect for a given shape. In turn, this can be used to develop estimators that are highly robust against high noise and occlusions.

I. INTRODUCTION

The idea of shape fitting is to find the set of shape parameters that best fit a list of given point measurements. In general, the shape is an extended object, or in other words, measurements are assumed to be generated from multiple point sources on the boundary of the shape. The problem is that, in general, these measurements are *noisy*, so that there is no guarantee that they lie on the boundary of the target shape. The usual approach to solve this issue is to associate each measurement in some way to sources on the shape, which allows for the derivation of a value or metric to be minimized or maximized.

Thus, shape fitting techniques can be categorized by taking into account two aspects: the shapes they consider, and the way they deal with the aforementioned *association problem*. For the first, there are approaches that deal with conics [1], [2], rectangles [3], line segments [3], and many others. For the second, we can subdivide this class into approaches that consider multiple sources probabilistically [3], [4], while others consider only a single best-fitting source [5], [6] which minimizes some metric. From the latter, a common approach is to minimize the sum of square Euclidian distances between measurements and their closest points [5], [7], also denoted as *least squares* approaches. As these techniques do not require a probabilistic modeling, they have the advantage of allowing for easier and robust implementations. However, as they do not exploit information about source selection and the noise characteristics, they have a problem of estimation bias [2], [8] that needs to be treated carefully, as it increases rapidly with high levels of noise.

In this paper we will address the problem of shape fitting using *Partial Information Models* [8]. The idea is that, by carefully reparametrizing the received measurements, we

can exploit *partial likelihoods* [9] in order to minimize the distances between measurements and the shape, while still taking into account noise properties and shape information. To achieve this, we will use *level-sets* to reconstruct the probability density of the distances we expect for a given shape in the presence of isotropic Gaussian noise. This allows for estimators that remove estimation bias almost completely while also remaining robust even in cases of very high noise.

This paper is structured in the following way. First, we will detail the problem formulation in Sec. II. Then, we will describe the shape models we will use for the derivation in Sec. III. After that, our contribution will be presented in Sec. IV. Following this, the implementation details will be explored in Sec. V. Sec. VI will present the evaluation, and then Sec. VII concludes the paper.

II. PROBLEM FORMULATION

In this work we are concerned with tracking an extended target shape, based on incoming point measurements $\mathcal{Y} = \{y_0, \dots, y_n\}$ in Cartesian coordinates. The boundary of the target shape is treated as the set of points \mathcal{S}_x , which we assume is a finite, closed and orientable curve. The parameters of this shape are contained in the state vector \underline{x} . Each measurement y_i is assumed to have been generated by the following random process. First, a measurement source $\underline{z}_i \in \mathcal{S}_x$ is selected from the shape boundary. Then, this source is corrupted by an additive noise term \underline{v}_i , which is Gaussian distributed in the form of

$$\underline{v}_i \sim \mathcal{N}(\underline{0}, \mathbf{C}_{v,i}), \quad (1)$$

yielding the measurement y_i . In this paper, we will focus on isotropic noise, i.e., $\mathbf{C}_{v,i} = \sigma_{v,i}^2 \cdot \mathbf{I}$, where $\sigma_{v,i}^2$ may be different for each measurement. Furthermore, we assume that the noise term \underline{v}_i is independent from the state and between measurements. Probabilistically, this generative model can be described using the probability density $p(y_i | \underline{x})$. For multiple measurements, we can extend this to

$$p(\mathcal{Y} | \underline{x}) = \prod_{i=0}^n p(y_i | \underline{x}), \quad (2)$$

which allows us to treat each measurement individually. In the following, the subindex i will be dropped unless needed.

III. SHAPE MODELS

A shape model describes the extended target \mathcal{S}_x , and more importantly, it tells us how to associate a measurement y to its possible sources. The main problem is that the true source is generally not known due to the noise term. This leads to an *association problem*, as we can only find how y is related to the state \underline{x} by associating it to one or more sources. For

¹The authors are with the Chair of Intelligent Sensor-Actuator-Systems (ISAS) at the Karlsruhe Institute of Technology (KIT). antonio.zea@kit.edu, florian.faion@kit.edu, uwe.hanebeck@ieee.org

simplicity, we will focus on curves in two-dimensional space, i.e., where sources and measurements are both in \mathbb{R}^2 .

In the following, we will discuss the parametric representation of the shape \mathcal{S}_x . Then, the remainder of this section will discuss how to deal with the measurement association.

A. Arc Length Parametrization

In order to discuss the shape \mathcal{S}_x , first we will need a proper way to describe all points that belong to the curve. Let $\underline{z}_x(s)$, for $s \in \mathbb{R}$, be an arbitrary regular arc length parametrization of the shape boundary (Fig. 1). Or in other words, $\underline{z}_x(s)$ is differentiable, does not jump backwards, and between $\underline{z}_x(0)$ and $\underline{z}_x(s)$ we will traverse an arc with length s . Hence, assuming that the \mathcal{S}_x has a total length of s_T , we can see that for $s \in [0, s_T]$ the function $\underline{z}_x(s)$ iterates through all possible sources. In the following, we will denote s as the *source parameter*.

For the mathematical derivation we will require the following properties of an arc length parametrization. It can be seen that $\underline{z}'_x(s)$, i.e., its derivative vector in function of s , determines the tangent at the position s . Analogously, we can define $\underline{n}_x(s)$ as the function which returns the normal at s , obtained by rotating $\underline{z}'_x(s)$ either $\frac{\pi}{2}$ or $-\frac{\pi}{2}$ so that it points outside. Furthermore, we can exploit the fact that \mathcal{S}_x is parametrized by arc length to obtain the following results. On the one hand, we know that $\|\underline{z}'_x(s)\| = 1$ for all s , where $\|\cdot\|$ is the Euclidian norm, from which it also follows that $\|\underline{n}_x(s)\| = 1$. On the other hand, it also holds that $\underline{n}'_x(s)$ is always orthogonal to $\underline{n}_x(s)$.

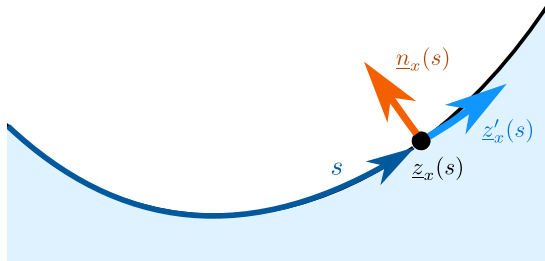


Fig. 1: Parametrization for the curve in black. For a given parameter s , the function $\underline{z}_x(s)$ selects the corresponding source. The tangent at this point is $\underline{z}'_x(s)$, and the normal is $\underline{n}_x(s)$ and points outwards. Light blue is the shape interior.

Thus, we can visualize the generative model from Sec. II in the following way. First, we randomly draw a parameter s according to a distribution $p(s|\underline{x})$ defined in $[0, s_T]$. This yields the source $\underline{z}_x(s)$. Second, this source is corrupted by the Gaussian noise term \underline{v} according to (1). From this, we obtain the measurement equation

$$\underline{y} = \underline{z}_x(s) + \underline{v}, \quad (3)$$

which, for a given s , can be described probabilistically as

$$p(\underline{y} | s, \underline{x}) = \mathcal{N}(\underline{y} - \underline{z}_x(s); \underline{0}, \mathbf{C}_v).$$

Note that the arc length representation is only important for the mathematical derivation. As we will see later, the implementation can use any arbitrary parametrization.

B. Spatial Distribution Model

A *Spatial Distribution Model* (SDM) [10] addresses the association problem by associating the measurement \underline{y} to all of its possible sources $\underline{z}_x(s)$, by marginalizing s in the form of

$$p(\underline{y} | \underline{x}) = \int_0^{s_T} \mathcal{N}(\underline{y} - \underline{z}_x(s); \underline{0}, \mathbf{C}_v) \cdot p(s | \underline{x}) \, ds. \quad (4)$$

Note, however, that this requires $p(s|\underline{x})$ to be explicitly known. Otherwise, a common approximation is to assume that sources are selected uniformly from \mathcal{S}_x , i.e., $p(s|\underline{x}) = \frac{1}{s_T}$ for $s \in [0, s_T]$.

C. Greedy Association Model

In many cases, such as when occlusions are present, there is no straightforward way to obtain $p(s|\underline{x})$, and an assumption of a uniform distribution may not yield good results. An alternative approach is to consider for each received measurement only a *single* source, i.e., the source which we believe to have generated it. As generally we cannot know the true source due to the noise term, we approximate it by the best-fitting source which minimizes some sort of distance metric. Thus, our approach is as follows. First, for a specific measurement \underline{y} , we find the best fitting source $\underline{\pi}_{\underline{y}}$. Then, we assume that $\underline{\pi}_{\underline{y}}$ is the true source, which allows us to derive a form of $p(\underline{y}|\underline{x})$ which exploits this information.

For this paper, the best-fitting source is defined as the *most likely* source, that is,

$$\underline{\pi}_{\underline{y}} := \arg \max_{\underline{z} \in \mathcal{S}_x} \mathcal{N}(\underline{y} - \underline{z}; \underline{0}, \mathbf{C}_v),$$

so that $\underline{\pi}_{\underline{y}}$ acts as some sort of *projection*. As we deal with isotropic noise, this is equivalent to

$$\underline{\pi}_{\underline{y}} = \arg \min_{\underline{z} \in \mathcal{S}_x} \|\underline{y} - \underline{z}\|^2, \quad (5)$$

i.e., the best-fitting source is the one that minimizes the Euclidian distance. We define $s_{\underline{y}}$ as the source parameter that generated $\underline{\pi}_{\underline{y}}$, or in other words, $\underline{\pi}_{\underline{y}} = \underline{z}_x(s_{\underline{y}})$. Finally, as we only assume $s_{\underline{y}}$ as a possible source parameter, it follows that $p(s|\underline{x}) \approx \delta(s - s_{\underline{y}})$, where $\delta(\cdot)$ is the Dirac-delta distribution. Plugging this on (4) leads to

$$\begin{aligned} p(\underline{y} | \underline{x}) &= \int_0^{s_T} \mathcal{N}(\underline{y} - \underline{z}_x(s); \underline{0}, \mathbf{C}_v) \cdot \delta(s - s_{\underline{y}}) \, ds \\ &= \mathcal{N}(\underline{y} - \underline{z}_x(s_{\underline{y}}); \underline{0}, \mathbf{C}_v) \\ &= \mathcal{N}(\underline{y} - \underline{\pi}_{\underline{y}}; \underline{0}, \mathbf{C}_v). \end{aligned} \quad (6)$$

as a result of the sifting property. This approach, denoted as a *Greedy Association Model* (GAM) [8], can be seen as a Bayesian interpretation of distance minimization approaches [3], [8].

The advantage of this mechanism is clear, as once the best-fitting source is found, $p(\underline{y}|\underline{x})$ can be obtained by a simple evaluation in a Gaussian distribution. Furthermore, unlike SDMs, there is no need to know the underlying $p(s|\underline{x})$.

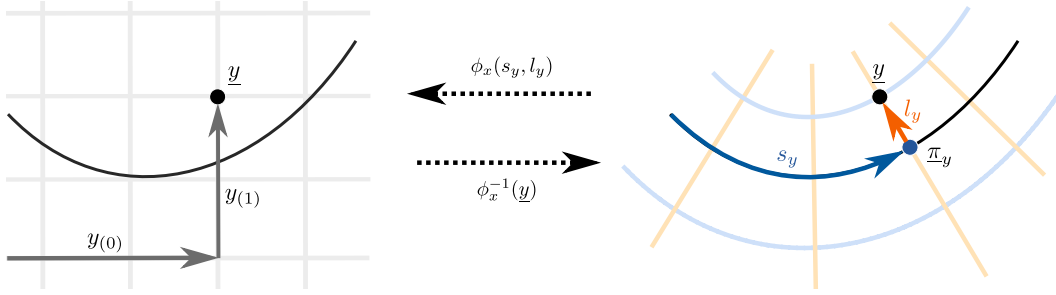


Fig. 2: Projection-based parametrization based on the curve shape in black. Left, a measurement \underline{y} is parametrized by its Cartesian coordinates $[y(0), y(1)]$. Right, we reparametrize \underline{y} as $[s_y, l_y]$, where s_y is the source parameter of the best-fitting source π_y , and l_y is the signed Euclidian distance.

This allows GAMs to be robust against occlusions and sensor artifacts, as we do not need to know a-priori which parts of the shape are visible to the sensor. However, this simplification comes with the caveat that it only considers the best-fitting source, which usually does *not* correspond to the true source. Thus, a GAM approach is only as good as its ability to discern what the true source was. This leads to estimation bias which increases with noise and shape curvature [2], [8]. It can be seen that we have two properties that appear to act against each other, unbiasedness and resistance to occlusion. In the following, we explore a new approach that aims to combine both strengths.

IV. PARTIAL INFORMATION MODEL

The key idea of *Partial Information Models* (PIMs) [8] is to minimize the effect of the unknown true source by finding a suitable parametrization ϕ_x of \underline{y} which divides it into two scalar components s_y and l_y . These values are related by

$$\underline{y} = \phi_x(s_y, l_y)$$

where s_y depends on $p(s | \underline{x})$ but l_y does not. If we assume that s_y and l_y are independent from each other, we can write

$$p(s_y, l_y | \underline{x}) = p(s_y | \underline{x}) \cdot p(l_y | \underline{x}). \quad (7)$$

Then, by applying the concept of *partial likelihood* [9], we ignore the s_y component and focus on the l_y component. Thus, instead of deriving $p(\underline{y} | \underline{x})$, we focus instead on

$$f(\underline{y} | \underline{x}) := p(l_y | \underline{x}). \quad (8)$$

As in (2), we can extend this to multiple measurements as

$$f(\mathcal{Y} | \underline{x}) = \prod_{i=0}^n f(\underline{y}_i | \underline{x}). \quad (9)$$

In practice, it is extremely difficult if not impossible to find a parametrization where (7) holds for arbitrary shapes. [8] proposed using a *projection-based* parametrization (Fig. 2) where s_y describes the best-fitting source, and l_y describing the so-called *signed* Euclidian distance to this source. While this approach does not make s_y and l_y fully independent from each other, even in the presence of isotropic noise, it reduces the correlation enough for (8) to yield good results. In the following, we will describe the proposed parametrization and then derive a formal description of $p(l_y | \underline{x})$.

A. Projection-based Parametrization

We are now interested in a function which produces a point \underline{p} from the scalars s_p and l_p . More formally, we relate an arbitrary point $\underline{p} \in \mathbb{R}^2$ to the scalars s_p and l_p by means of the function $\phi : [0, s_T] \times \mathbb{R} \rightarrow \mathbb{R}^2$, defined as

$$\underline{p} = \phi_x(s_p, l_p) := \underline{z}_x(s_p) + l_p \cdot \underline{n}_x(s_p),$$

that is, \underline{p} is obtained by selecting the source corresponding to s_p , and then adding the normal at that point scaled by l_p . We are interested in two aspects of this function, its Jacobian matrix and its inverse. The Jacobian matrix of $\phi_x(\cdot, \cdot)$, which we will later require in order to use the change-of-variables technique, has the form

$$\begin{aligned} \mathbf{J}_\phi(s_p, l_p) &:= \begin{bmatrix} \frac{\partial \phi}{\partial s_p}(s_p, l_p), & \frac{\partial \phi}{\partial l_p}(s_p, l_p) \end{bmatrix} \\ &= \begin{bmatrix} \underline{z}'_x(s_p) + l_p \cdot \underline{n}'_x(s_p), & \underline{n}_x(s_p) \end{bmatrix}. \end{aligned}$$

We observe that both columns are orthogonal to each other, as both $\underline{z}'_x(s_p)$ and $\underline{n}'_x(s_p)$ are orthogonal to $\underline{n}_x(s_p)$ (see Sec. III-A). Thus, the determinant of the Jacobian matrix has the form

$$\begin{aligned} \det(\mathbf{J}_\phi(s_p, l_p)) &= \left\| \frac{\partial \phi}{\partial s_p}(s_p, l_p) \right\| \cdot \left\| \frac{\partial \phi}{\partial l_p}(s_p, l_p) \right\| \\ &= \left\| \frac{\partial \phi}{\partial s_p}(s_p, l_p) \right\|, \end{aligned}$$

as the norm of the partial derivative for l_p is always 1. The inverse has the form

$$\begin{bmatrix} s_p \\ l_p \end{bmatrix} = \phi_x^{-1}(\underline{p}),$$

where s_p and l_p are obtained in the following way. On the one hand, s_p can be calculated as the source parameter that corresponds to its best-fitting source π_p , as we did in Sec. III-C. On the other hand, l_p represents the signed Euclidian distance $d_x^\phi(\underline{p})$ to this source, defined as

$$d_x^\phi(\underline{p}) := \begin{cases} \|\underline{p} - \pi_p\| & \text{if } \underline{p} \text{ outside } \mathcal{S}_x \\ -\|\underline{p} - \pi_p\| & \text{otherwise.} \end{cases} \quad (10)$$

For the sake of formality, we see that multiple pairs of $[s_p, l_p]$ may produce the same point \underline{p} . In order to ensure that ϕ remains invertible, we will only consider as valid the pair with the smallest $|l_p|$.

B. Deriving a Measurement Equation for PIMs

By applying ϕ_x^{-1} to both sides of (3) we obtain the new measurement equation

$$\begin{bmatrix} s_y \\ l_y \end{bmatrix} = \phi_x^{-1}(\underline{z}_x(s) + \underline{v}). \quad (11)$$

As a short reminder, s_y is the source parameter of the best-fitting source of \underline{y} , and s is the parameter for the source we are associating \underline{y} with. From (11) we are particularly interested in the part which is related to l_y , or in other words, we want to derive $p(l_y | \underline{x})$ from

$$l_y = d_x^\phi(\underline{z}_x(s) + \underline{v}).$$

The approach we will use works as follows. First, for a given s , we describe (11) probabilistically as

$$\begin{aligned} p(s_y, l_y | s, \underline{x}) &= p(\underline{y} | s, \underline{x}) \cdot \det(\mathbf{J}_\phi(s_y, l_y)) \\ &= \mathcal{N}(\phi_x(s_y, l_y) - \underline{z}_x(s); \underline{0}, \mathbf{C}_v) \cdot \left\| \frac{\partial \phi}{\partial s_p}(s_y, l_y) \right\| \end{aligned}$$

by applying the change-of-variables technique. In a similar fashion as SDMs in (4), we obtain the following density by marginalizing out s ,

$$p(s_y, l_y | \underline{x}) = \int_0^{s_T} p(s_y, l_y | s, \underline{x}) \cdot p(s | \underline{x}) \, ds. \quad (12)$$

Finally, by also marginalizing out s_y , we obtain

$$p(l_y | \underline{x}) = \int_0^{s_T} p(s_y, l_y | \underline{x}) \, ds_y. \quad (13)$$

However, it becomes clear that this term is generally untractable, in particular due to the evaluation of two integrals. Furthermore, it still requires an a-priori knowledge of $p(s | \underline{x})$. In the following, we will simplify this model using ideas from GAMs.

C. Simplifying the Model

In a similar way as we did with GAMs in (6), we remove the dependency on $p(s | \underline{x})$ by considering only the best-fitting source. Thus, given a measurement $\tilde{\underline{y}}$, we consider that the only possible source is $\underline{\pi}_{\tilde{\underline{y}}}$, yielding

$$\begin{bmatrix} s_y \\ l_y \end{bmatrix} = \phi_x^{-1}(\underline{\pi}_{\tilde{\underline{y}}} + \underline{v}),$$

from which we are interested particularly in the term

$$l_y = d_x^\phi(\underline{\pi}_{\tilde{\underline{y}}} + \underline{v}). \quad (14)$$

As we only consider a single source, $p(s | \underline{x})$ is reduced again to a Dirac, which reduces (12) to a simple evaluation in a Gaussian distribution in the form of

$$p(s_y, l_y | \underline{x}) = \mathcal{N}(\phi_x(s_y, l_y) - \underline{\pi}_{\tilde{\underline{y}}}; \underline{0}, \mathbf{C}_v) \cdot \left\| \frac{\partial \phi}{\partial s_y}(s_y, l_y) \right\|.$$

By plugging this term in (13), we obtain

$$p(l_y | \underline{x}) = \int_0^{s_T} \mathcal{N}(\phi_x(s_y, l_y) - \underline{\pi}_{\tilde{\underline{y}}}; \underline{0}, \mathbf{C}_v) \cdot \left\| \frac{\partial \phi}{\partial s_y}(s_y, l_y) \right\| \, ds_y.$$

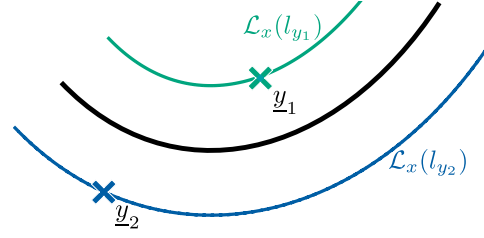


Fig. 3: For the given curve (black), the level-set $\mathcal{L}_x(l_{y_1})$ (green) contains \underline{y}_1 and all other points with the signed Euclidean distance l_{y_1} to the shape. Similarly, $\mathcal{L}_x(l_{y_2})$ (blue) contains all points with signed Euclidean distance l_{y_2} .

D. PIMs as Line Integrals

An interesting fact of $p(l_y | \underline{x})$ is that it has the form of a *line integral*. By considering all $s_y \in [0, s_T]$, the term $\phi_x(l_y, s_y)$ traverses the curve formed by all points whose signed Euclidean distance to \mathcal{S}_x is equal to l_y . This curve is the level-set

$$\mathcal{L}_x(l_y) := \{ \underline{p} \in \mathbb{R}^2 \mid d_x^\phi(\underline{p}) = l_y \},$$

visualized in Fig. 3. By using a change of variables, we can use *any* smooth parametrization of $\mathcal{L}_x(l_y)$ without changing the result. For example, let us consider an arbitrary function $\underline{r}(\hat{s}) : [\hat{s}_0, \hat{s}_1] \rightarrow \mathbb{R}^2$ that describes the same level-set. Then, we can also write

$$p(l_y | \underline{x}) = \int_{\hat{s}_0}^{\hat{s}_1} \mathcal{N}(\underline{r}(\hat{s}) - \underline{\pi}_{\tilde{\underline{y}}}; \underline{0}, \mathbf{C}_v) \cdot \|\underline{r}'(\hat{s})\| \, d\hat{s}, \quad (15)$$

where $\underline{r}'(\hat{s})$ represents the derivative vector.

At this point, we see that the arc length parameter s and the parametrization $\underline{z}_x(s)$, which are usually difficult to calculate, are not needed anymore. Instead, an implementation only requires $\underline{\pi}_{\tilde{\underline{y}}}$ and can use any arbitrary parametrization of $\mathcal{L}_x(l_y)$.

V. IMPLEMENTATION USING POLYGONS

Given the theoretical derivation presented in Sec. IV, we now want to consider the practical aspects of the implementation. To recapitulate, a PIM works as follows. Given a measurement $\tilde{\underline{y}}$, we

- 1) find the best-fitting source $\underline{\pi}_{\tilde{\underline{y}}}$ of $\tilde{\underline{y}}$ as shown in (5),
- 2) calculate $l_{\tilde{\underline{y}}} = d_x^\phi(\tilde{\underline{y}})$ using (10), then finally
- 3) obtain the distribution $p(l_y | \underline{x})$ that arises from (14), calculated using (15).

The most difficult tasks are finding $\underline{\pi}_{\tilde{\underline{y}}}$ and constructing $p(l_y | \underline{x})$. In this section we will describe an approach to obtain these terms for general shapes, with focus on circles, by using polygonal shapes.

A. Best-Fitting Sources

For a circle with center \underline{c}_x and radius r_x , the best-fitting source of $\tilde{\underline{y}}$ can be obtained easily from

$$\underline{\pi}_{\tilde{\underline{y}}} = \underline{c}_x + \frac{\tilde{\underline{y}} - \underline{c}_x}{\|\tilde{\underline{y}} - \underline{c}_x\|} \cdot r_x.$$

For general shapes, we can assume that they can be approximated using the polygon $\mathcal{A}_x^s = \{\underline{a}_0^s, \dots, \underline{a}_m^s\} \in \mathbb{R}^{2 \times m}$. For each segment connecting the vertices \underline{a}_i^s and \underline{a}_{i+1}^s we define a *candidate* point as

$$\underline{\pi}_{\tilde{y},i}^c := \underline{a}_i^s + \text{clamp}(t_i) \cdot (\underline{a}_{i+1}^s - \underline{a}_i^s) ,$$

where $\text{clamp}(t_i) := \max(\min(t_i, 1), 0)$ and

$$t_i := \frac{\tilde{y} - \underline{a}_i^s}{\|\underline{a}_{i+1}^s - \underline{a}_i^s\|^2} .$$

Finally, from each of the found candidates $\underline{\pi}_{\tilde{y},i}^c$ we select the one with the smallest Euclidian distance to \tilde{y} as the best-fitting source $\underline{\pi}_{\tilde{y}}$.

B. Constructing the Level-Sets

In order to calculate $p(l_y | \underline{x})$, we need to construct the level-set that corresponds to l_y . For circles, the construction is straightforward, as the level-set $\mathcal{L}_x(l_y)$ of a circle of radius r_x is another circle with the same center and radius $r_x + l_y$. For arbitrary shapes, however, the explicit construction of a level-set may be difficult. Approaches to find these can be found in literature such as [11]. Once the level-set is available, we can calculate $p(l_y | \underline{x})$ easily using the following approach. First, we approximate the level-set $\mathcal{L}_x(l_y)$ as the polygonal shape \mathcal{A}_x^l . Then, we obtain a solution by using

$$p(l_y | \underline{x}) \approx L_p(\underline{\pi}_{\tilde{y}}, \mathcal{A}_x^l, \mathbf{C}_v) ,$$

where $L_p(\cdot, \cdot, \cdot)$ is the integral of a Gaussian distribution over the polygonal segments.

C. Gaussian Approximation of $p(l_y | \underline{x})$

An alternative to explicitly calculating $p(l_y | \underline{x})$ was proposed in [8] by means of a Gaussian distribution. The idea is, for a given \underline{x} , to calculate the mean and variance of l_y in the form of

$$\begin{aligned} \bar{l}_y &= \mathbb{E} \left[d_x^\phi(\underline{\pi}_{\tilde{y}} + \underline{v}) \right] \\ \sigma_{l_y}^2 &= \mathbb{E} \left[(d_x^\phi(\underline{\pi}_{\tilde{y}} + \underline{v}) - \bar{l}_y)^2 \right] , \end{aligned}$$

which allows us to construct a Gaussian approximation by moment matching, given by

$$p(l_y | \underline{x}) \approx \mathcal{N}(l_y; \bar{l}_y, \sigma_{l_y}^2) .$$

As these values generally cannot be obtained analytically, they are approximated by means of sample propagation. The advantage of this approach is that it avoids the explicit construction of level-sets required by (15). However, it should be noted that for higher noise levels, a Gaussian distribution generally stops being an appropriate fit for $p(l_y | \underline{x})$.

D. Developing an Estimator

By assuming that \mathcal{Y} is fixed and \underline{x} is a free variable, we can interpret (9) as a likelihood function. This allows us to use stochastic approaches to estimate the parameter vector \underline{x} . Thus, a *maximum likelihood* (ML) estimate is obtained from

$$\underline{x}_{ML} = \arg \max_{\underline{x}} f(\mathcal{Y} | \underline{x}) . \quad (16)$$

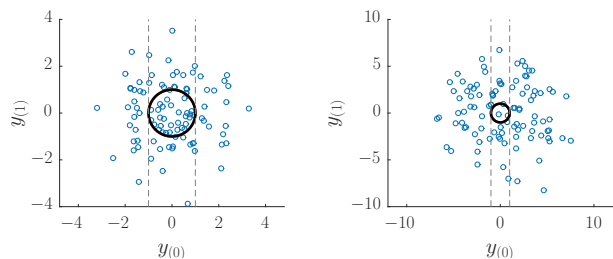
Furthermore, a recursive Bayesian estimator can be used to *update* an estimate of \underline{x} , described with the prior distribution $f^p(\underline{x})$, in the form of

$$f^e(\underline{x} | \mathcal{Y}) = c \cdot f(\mathcal{Y} | \underline{x}) \cdot f^p(\underline{x}) ,$$

where c is a normalization constant, and $f^e(\underline{x})$ is the posterior distribution. Coupled with a dynamic model, a Bayesian estimator can also incorporate information about changes in time and *predict* the state to a subsequent time step. However, for the evaluation we will focus on (16).

VI. EVALUATION

In this section we will evaluate the proposed PIM approach. First, we will examine how the likelihood functions of selected state-of-the-art techniques behave for different noise levels. Then, we will compare these techniques in fitting scenarios using circles. As an evaluation for relatively low noise was already performed in [8], in this paper we want to explore higher noise levels to test the limitations of the proposed approaches. Fig. 4 shows example measurements and their spread in relation to the size of the considered shapes.



(a) Example measurements $\sigma_v = 1$. (b) Example measurements $\sigma_v = 3$.

Fig. 4: Experiment setup with example measurements. The dotted vertical lines at -1 and 1 help visualize the bounds of the ground truth circle with radius $r_x = 1$.

A. Circle Likelihood Functions

In the following, we want to compare four approaches for fitting a circle. The first one is *PIM-LS*, i.e., the PIM using level-sets as described in Sec. V-B. Then, the second one is *PIM-Gauss*, which uses the Gaussian approximation explained in Sec. V-C with 31 samples. Third, we wanted to compare the approach proposed by *Okatani* et al. [2]. For this approach, given a circle with radius r_x , we use the approximation

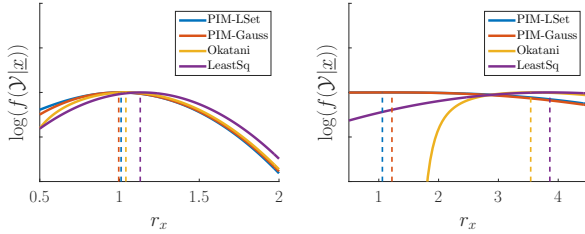
$$p(l_y | \underline{x}) \approx \mathcal{N} \left(l_y; \eta_x, \sigma_v^2 \cdot (1 - \eta_x^2)^2 \right) ,$$

with $\eta_x := \frac{\sigma_v^2}{2r_x}$. Finally, the *Least Squares* approach assumes

$$p(l_y | \underline{x}) \approx \mathcal{N}(l_y; 0, \sigma_v^2) . \quad (17)$$

It can be seen that maximizing the product of likelihoods from (17) is equivalent to minimizing the sum of their corresponding squared Euclidian distances l_y^2 . For reference, the ground truth circle has a radius of $r_x = 1$.

When fitting circles to measurements without occlusions, it is commonly the case that the center can be easily found



(a) Likelihoods for $\sigma_v = 0.5$. (b) Likelihoods for $\sigma_v = 3$.

Fig. 5: Likelihood functions for \mathcal{Y} with different noise levels. Dotted vertical lines show the r_x which yield the ML.

but the radius estimate is biased. Thus, for this experiment, we are only interested in estimating the radius x_r of a circle whose center is fixed at the origin. Fig. 4 shows the setup and example measurements. Then, we generated a set \mathcal{Y} of 10^5 measurements from sources which were drawn uniformly from the circle, and we multiplied their likelihoods as shown in (9) to obtain the corresponding likelihood functions for \mathcal{Y} . Note that we used a high amount of measurements because we wanted to obtain the best possible results each estimator could provide. The results are shown in Fig. 5. It can be seen that PIM-LSet, PIM-Gauss, and Okatani are almost identical for low noise levels, as the Gauss approximation is a good fit for $p(l_y | \underline{x})$. However, as noise increases, Okatani encounters a singularity and becomes heavily biased. The Least Squares approach is observed to consistently return the worst results.

B. Circle Fitting with ML

Next, we wanted to compare the four approaches when the center was also being estimated. Thus, the state had the form $\underline{x} = [\underline{c}_x, r_x]^T$, where \underline{c}_x was the circle center. In addition, we also wanted to evaluate the effect of occlusions, and for this we only generated sources uniformly in the range of $[0, \alpha]$. Fig. 6 shows the ML results after 10^5 measurements. To obtain these maxima we used the MATLAB function `fminsearch` with default parameters and a starting estimate of $[3, 3, 3]^T$. For reference, the ground truth was $[0, 0, 1]^T$. In cases of occlusion, we see that the center estimate was biased in a direction opposite to the missing sources. Otherwise, as expected, the center was found by all estimators even with high noise. For the radius, however, Okatani and Least Squares were once again highly biased. The PIM approaches could still estimate the radius appropriately, even with a high noise variance of $\sigma_v^2 = 36$.

VII. CONCLUSIONS

In this paper, we presented an implementation of Partial Information Models. The idea was to reparametrize measurements in function of their best-fitting source and their distance to the shape, which allowed for the derivation of a partial likelihood which reduced the effect of the association problem. Then, using level-sets, we derived a mechanism to closely approximate the distribution of distances we expect

for a given shape. Using this information, we developed a maximum likelihood estimator which was able to estimate shapes, in particular circles, in the presence of occlusions and extremely high noise levels. We compared our estimator with other state-of-the-art approaches to demonstrate its high robustness and low estimation bias.

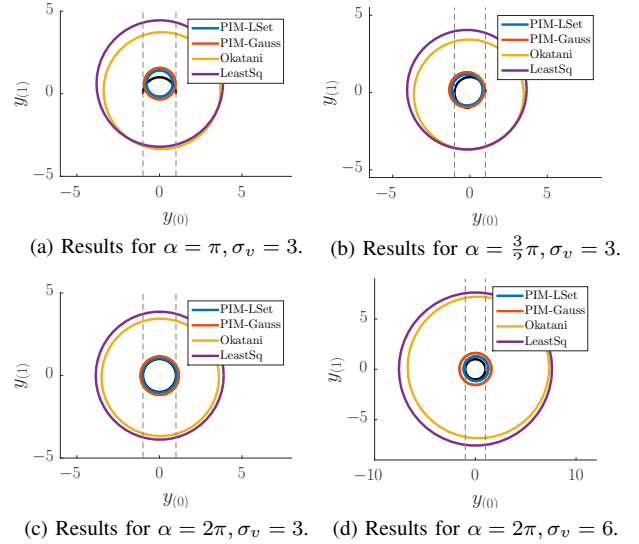


Fig. 6: Results for different noise levels, using a circle (black) that only generates measurements in an arc between $[0, \alpha]$.

REFERENCES

- [1] M. Baum and U. D. Hanebeck, "Fitting Conics to Noisy Data Using Stochastic Linearization," in *Proceedings of the 2011 IEEE/RSJ International Conference on Intelligent Robots and Systems (IROS 2011)*, San Francisco, California, USA, Sep. 2011.
- [2] T. Okatani and K. Deguchi, "On bias correction for geometric parameter estimation in computer vision," in *Computer Vision and Pattern Recognition, 2009. CVPR 2009. IEEE Conference on*. IEEE, 2009, pp. 959–966.
- [3] M. Werman and D. Keren, "A Bayesian method for fitting parametric and nonparametric models to noisy data," *IEEE Transactions on Pattern Analysis and Machine Intelligence*, vol. 23, no. 5, pp. 528–534, 2001.
- [4] K. Gilholm and D. Salmund, "Spatial distribution model for tracking extended objects," in *Radar, Sonar and Navigation, IEE Proceedings-*, vol. 152, no. 5. IET, 2005, pp. 364–371.
- [5] W. Gander, G. H. Golub, and R. Strebler, "Least-squares fitting of circles and ellipses," *Bulletin of the Belgian Mathematical Society Simon Stevin*, vol. 3, no. 5, pp. 63–84, 1996.
- [6] P. Lancaster and K. Salkauskas, "Curve and surface fitting. an introduction," *London: Academic Press*, 1986, vol. 1, 1986.
- [7] A. Fitzgibbon, M. Pilu, and R. B. Fisher, "Direct least square fitting of ellipses," *Pattern Analysis and Machine Intelligence, IEEE Transactions on*, vol. 21, no. 5, pp. 476–480, 1999.
- [8] F. Faion, A. Zea, M. Baum, and U. D. Hanebeck, "Partial Likelihood for Unbiased Extended Object Tracking (to appear)," in *Proceedings of the 18th International Conference on Information Fusion (Fusion 2015)*, Washington D. C., USA, Jul. 2015.
- [9] D. R. Cox, "Partial likelihood," *Biometrika*, vol. 62, no. 2, pp. 269–276, 1975.
- [10] K. Gilholm and D. Salmund, "Spatial Distribution Model for Tracking Extended Objects," *IEE Proceedings on Radar, Sonar and Navigation*, vol. 152, no. 5, pp. 364–371, 2005.
- [11] S. Osher and R. Fedkiw, *Level set methods and dynamic implicit surfaces*. Springer Science & Business Media, 2003, vol. 153.